Zoological Journal of the Linnean Society, 2022, **195**, 88–105. With 3 figures.

Metric variation in the postcranial skeleton of ostriches, *Struthio* (Aves: Palaeognathae), with new data on extinct subspecies

ANDRZEJ ELZANOWSKI[1,*] and ANTOINE LOUCHART[2]

[1]*Department of Liberal Arts, University of Warsaw, 72 Dobra Street, 00-312 Warszawa, Poland*
[2]*Univ Lyon, UCBL, ENSL, UJM, CNRS, LGL-TPE, F-69622, Villeurbanne, France*

Received 16 January 2021; revised 15 May 2021; accepted for publication 14 June 2021

As a result of numerous fossil and subfossil finds of ostriches, there is great demand for a comprehensive osteometric dataset for the living species and subspecies of the genus *Struthio*. We meet this demand by providing a set of > 100 measurements for a sample of 18 sexed skeletons, including all living and recently extinct species and subspecies of ostriches. We provide the first mensural data for two extinct subspecies, the hitherto questioned *Struthio camelus spatzi* from north-western Africa and the Arabian ostrich, *Struthio camelus syriacus*. The unique skeletal proportions of *S. c. spatzi*, with a relatively short wing, broad pelvis, short tarsometatarsus and big third toe, confirm the validity of this taxon and suggest an increased stability at the expense of cursoriality, which might have contributed to its extermination by humans. Our biometric analysis of the entire sample suggests a subtle sexual dimorphism in the ostrich skeleton, with females having more robust limb bones (especially wider and/or deeper at the ends) despite being on average smaller than males. If confirmed by further research, this size-independent dimorphism might reflect the independent regulation of the longitudinal and transverse dimensions of bones as revealed by several independent studies of morphological integration (covariance among morphological traits) in the avian skeleton.

ADDITIONAL KEYWORDS: Anthropocene extinction – Arabian ostrich – highland ostrich – morphological integration – Palaeognathae – pedal digit – pelvic limb – sexual dimorphism – *Struthio camelus spatzi* – *Struthio camelus syriacus*.

INTRODUCTION

Two living species of ostriches (*Struthio* Linnaeus, 1758), the genus comprising the largest living birds, are currently recognized (Folch *et al.*, 2020): the common ostrich, *Struthio camelus* Linnaeus, 1758, with three living and one extinct subspecies (*Struthio camelus syriacus* Rothschild, 1919), and the monotypic blue-necked (Somali) ostrich, *Struthio molybdophanes* Reichenow, 1883, recently elevated among many other subspecies to the species rank by Del Hoyo & Collar (2014) following its divergence in both mitochondrial and microsatellite nuclear sequences (Miller *et al.*, 2011). Among the subspecies of *S. camelus*, the southern ostrich, *Struthio camelus australis* Gurney, 1868, is closest to the Masai ostrich, *Struthio camelus massaicus* Neumann, 1898, and the red-necked ostrich, *Struthio camelus camelus* Linnaeus, 1758, to the extinct Arabian ostrich, *S. c. syriacus* (Robinson & Matthee, 1999; Miller *et al.*, 2011). Subspecies might differ slightly in body proportions, with *S. c. australis* considered to be the heaviest (males ≤ 150 kg) but not tallest race (Brown *et al.*, 1982). However, no exact data are available. Body mass in *S. c. massaicus* ranges from 86 to 145 kg (Davies, 2002). At least in *S. c. camelus* the females are shorter and lighter than the males, at 175–190 vs. 210–275 cm tall, respectively (Cramp & Simmons, 1977) and 90–110 vs. 100–130 kg body mass (Davies, 2002). The extreme values without subspecies identification are 64 kg for a female and 156.8 kg for a male (Davies, 2002). Juveniles reach the adult height at 1 year of age, but reach adult body mass only at 18 months and sexual maturity at the age of 3–4 years (Cramp & Simmons, 1977; Folch, 1992; Davies, 2002: 269).

*Corresponding author. E-mail: elzanowski@al.uw.edu.pl

Although length measurements, primarily of the pelvic limb bones, have been published occasionally (Lowe, 1931; Schaller *et al.*, 2005), there is a great demand for a comprehensive osteometric dataset based on all living ostriches as a reference for the identification of numerous ostrich fossils that usually differ only in size and proportions. Only Burchak-Abramovich (1953) provided many measurements in addition to length for between six and 12 (depending on the bone) specimens, although without sex and (except for two specimens) subspecies data, and with some of them (including the only specimen identified as *S. molybdophanes*) being obviously immature. Given that the osteometric reference for comparisons with fossil and, especially, subfossil ostriches should take both (sub)species and sex differences into account, we searched for skeletal specimens of extant ostriches with both types of data. Unexpectedly, the task proved difficult, because the majority of ostrich skeletons in the available collections (including some of the largest) do not have subspecies information, many specimens (including those in African museums) come from indeterminate hybrids that stem from more than a century of ostrich farming (Petitte & Davis, 1999), and few have both types of data. Our sample might well approach the maximum number of sexed ostrich skeletons with subspecies data that can be assembled, at least from the European collections (and possibly even worldwide), but remains too small to analyse possible differences between subspecies. However, it provides the first and by far the best referential dataset to date for comparisons with fossil specimens, and it allows us to define the skeletal proportions of two extinct subspecies, the Arabian ostrich *S. c. syriacus* and the hitherto disputed *Struthio camelus spatzi* Stresemann, 1926.

Using our dataset of nearly all possible measurements of the appendicular skeleton, we found the first evidence for unexpected size-independent sexual dimorphism in the ostriches that affects primarily the transverse dimensions of limb bones. Studies of sexual dimorphism in the avian skeleton have been limited largely to the length of limb bones that are correlated with size dimorphism, as in the moas (Bunce *et al.*, 2003; Olson & Turvey, 2013), mihirungs, Dromornitidae (Handley, 2016) and a few neognaths, including steamer ducks, *Tachyeres* Owen, 1875 (Livezey & Humphrey, 1986), common eiders, *Somateria mollissima* (Linnaeus, 1758) (Ericson, 1987), Eurasian cranes, *Grus grus* (Linnaeus, 1758) (Stewart, 2007), owls (Winde, 1977) and diurnal raptors (Bährmann 1974; Solti, 1996). Preliminary data on size dimorphism of the skeleton in the anatids, phasianids, owls and accipitrids have been gathered in the Munich school dissertations listed by Stewart (2007: 21). Aside from qualitative differences attributable to sexual selection, such as the presence of tarsal spurs in the males of many Phasianidae (Davison, 1985; Sullivan & Hillgarth, 1993), size-independent dimorphism in the postcranial skeleton is so far known to occur only in the foot of some birds, including galliforms and passerines, in which pedal digit ratios II/III and II/IV of the females are lower compared with those of the males (Navarro *et al.*, 2007; Saino *et al.*, 2007; Leoni *et al.*, 2008), and in the legs of burrowing owls, *Speotyto cunicularia* (Molina, 1782), in which the females have shorter tarsi even though they are larger than the males (Plumpton & Lutz, 1994).

Size-independent sexual dimorphism is better documented in avian skulls, primarily in the size and shape of the jaws. Females of some birds of paradise (Paradisaeidae) have longer bills, although they are smaller than the males (Frith, 1997). In green woodhoopoes, *Phoeniculus purpureus* (J.F. Miller, 1784), the slightly larger males have disproportionately larger bills, and the difference is maintained by natural selection (Radford & du Plessis, 2004), which might also be true of some species of hummingbirds, with slightly larger females having longer or more curved bills (Berns & Adams, 2010; Temeles *et al.*, 2010). Qualitative, and thus prima facie size independent, are the extreme sexual dimorphism in the size and shape of the bill in the extinct huia, *Heteralocha acutirostris* (Gould, 1837) (Lambert *et al.*, 2009), and the presence of cranial humps in the male but not female scoters, *Melanitta* F. Boie, 1822, whereas sexual differences in size of the cranial protuberances in at least six other species of Anatidae and *Anseranas* Lesson, 1828 are size dependent (Mayr, 2018). Male eagle-owls, *Bubo bubo* (Linnaeus, 1758), have broader skulls (braincases) than the females that are otherwise larger (McGillivray, 1985).

MATERIAL AND METHODS

Institutional abbreviations

IRSNB, Institut Royal des Sciences Naturelles de Belgique, Brussels, Belgium; ISEA, Instytut Systematyki i Ewolucji Zwierząt, Kraków, Poland; NHMUK, National History Museum, Tring, UK; OUMNH, Oxford Unversity Museum of Natural History, Oxford, UK; SAM, Iziko South African Museum, Cape Town, South Africa; SAPM, Staatssammlung für Anthropologie und Paläoanatomie München, Munich, Germany; USNM, National Museum of Natural History, Smithsonian Institution, Washington, DC, USA; ZMB, Museum für Naturkunde, Berlin, Germany.

Measurements

Altogether, we measured 18 sexed skeletons, ten males and seven females, from seven collections (Supporting Information, Table S1). Subspecies/species identification was available for 13 specimens: one *S. c. australis*, three *S. c. camelus*, two *S. c. massaicus*, three *S. molybdophanes*, two *S. c. syriacus* and one *S. c. spatzi*. We took ≤ 128 measurements (Table 1; Fig. 1) from each skeleton, although for most skeletons this number was closer to 100 because of the lack of distal pedal phalanges and sometimes other elements. Measurements of paired elements were recorded separately and averaged. Each measurement was taken at least three times using standard-size callipers (for most measurements) and macrocallipers (Sylvac ULIII) for the largest distances.

In order to promote standardization of osteological measurements, which should make them more useful for comparative research and more easily repeatable by others, and to reduce the need to define and illustrate them each time (except for special cases), we propose to categorize them into two types, as either defined-point or orthogonal measurements. A defined-point measurement is the distance connecting two predefined terminal points, which must be grasped between the opposite points of calliper jaws. An orthogonal measurement is the distance between two parallel planes of the planar grasping surfaces of the calliper jaws, which grasp the most projecting points irrespective of their mutual position on the opposite planes, without the need for specifying any terminal points beforehand. A clear distinction between these two types is necessary for the precision and repeatability of osteological measurements. The most common orthogonal measurements are axial measurements of long bones; that is, otherwise unspecified length, width and depth, all of which ultimately rely on the determination of the long axis. Unless specified otherwise, the term length means a distance between two parallel planes that are perpendicular to the long axis of a bone and cross its extreme points. Unless specified otherwise, the term width is used consistently for a mediolateral, and the term depth for a craniocaudal (as in stylopodia and zeugopodia), dorsoventral or dorsoplantar (as in autopodia) distance between planes that, for both measurements, are parallel to the long axis, but perpendicular to each other. Width and depth are here referred to jointly as transverse measurements. We also used other orthogonal measurements, such as diameters, which are distances between two parallel tangent planes. However, given that bones have curvilinear and often irregular shapes and that their axes can only be approximated, some of the measurements are defined as the minimum or maximum, commanding a search for the shortest or the longest distance within the limits of a geometric definition. This categorization is in terms of measuring practice as imposed by the special properties of bones.

Owing to the low numbers of sexed specimens, the differences between males and females were tested using a non-parametric Mann–Whitney *U*-test, with the software PAST (Hammer *et al.*, 2001). In PAST3, we selected 'Univariate: two sample tests: Mann-Whitney *U*-test', and retained the *U*-value and the *P*-value with 'exact permutation'. Sexual dimorphism was recognized when $P < 0.05$, but also a few cases with near-significant values of $0.05 < P < 0.1$ were considered. Owing to the small sample size, we provide the median and the minimum–maximum range as the most reliable result for each measurement. However, we also used the mean values for all wild-collected specimens in order to calculate coefficients of variation (CVs) and compare them with literature data, and the mean values for all males and all females, which were used to calculate Storer's indices (Storer, 1966) only for the measurements that proved sexually dimorphic in Mann–Whitney *U*-tests tests (significant or near-significant). It was not possible to test for differences between the two currently recognized living species of ostriches and among the subspecies of *S. camelus* because of the low numbers of specimens with species/subspecies identification. However, we could define clear differences in proportions and/or size between all the living ostriches and specimens of the two extinct taxa.

RESULTS

Extinct ostriches

The measurements of the appendicular skeleton in a sample comprising specimens from all extant and recently extinct species-level taxa of ostriches are provided in the Supporting Information (Tables S2–S16). Except for a few measurements of pelvis and femoral length taken by Lowe (1931), we provide the first skeletal measurements for the extinct Arabian ostrich, *S. c. syriacus*, which are derived from two male specimens at the Natural History Museum, Tring, UK (Supporting Information, Table S1), which are probably the only almost complete skeletal specimens of this subspecies available in collections worldwide (Trombone, 2013). Unfortunately, one of them (NHMUK 1923.6.10.1) is incompletely ossified and the other (NHMUK 1924.4.8.1) is somewhat damaged.

The length measurements in *S. c. syriacus* are lower than the means for the males of living ostriches for the wing bones by 8–16.5% and for the femur,

Table 1. Measurements of the appendicular skeleton and synsacrum in ostriches (*Struthio*), in the order of their left-to-right sequence in the Supporting Information (Tables S2–S16)

Bone	Abbreviation and definition	Type
Scapulocoracoid (Fig. 1A)	L_T, total length, perpendicular to the sternal margin	Orthogonal
	W_{St}, sternal width, between the tips of medial and lateral angles of the sternal margin	Defined point
Sternum (Fig. 1B)	W_{Is}, interspinal width between the lateral margins of the spinae sternocoracoideae	Defined point
	W_{Pc}, postcostal width, minimum, between dorsal edges, at the narrowest point behind the ribs	Defined point
Humerus	L_v, ventral length between ventral tubercle and ventral condyle	Defined point
	W_d, distal width between the epicondyles (oblique)	Defined point
Ulna, radius, carpometacarpus, manual digit II phalanx 1	L_T, total length, parallel to the long axis	Orthogonal
Synsacrum (Fig. 1C)	L_M, midline length, ventrally between the (concave) cranial facet of vertebra 1 corpus and caudal margin of the last synsacral vertebra*	Defined point
	L_C, midline corpus length, ventrally	Defined point
	W_C, corpus width, minimum	Orthogonal
	D_T, total depth (including spinal process)	Orthogonal
	W_{par}, the span of parapophyses	Defined point
	W_{prz}, the span of praezygapophyses	Defined point
Pelvis (Fig. 1C)	L_L, lateral length, minimum, between the anterior embayment of the ala praeacetabularis and the tip of spina dorsolateralis ilii	Defined point
	L_{PA}, preangular length†, minimum, between the cranial embayment of the ala praeacetabularis and the angulus ilii	Defined point
	L_{PO}, postangular length†, maximum, between the angulus ilii and the tip of spina dorsolateralis ilii	Defined point
	W_{PrA}, preacetabular width, minimum	Orthogonal
	W_{Ant}, antitrochanteric width between the outermost points of antitrochanters‡, maximum	Defined point
	W_{Ang}, angular width between the anguli ilii	Defined point
	W_{PoA}, postacetabular width (close to the caudal end), minimum	Orthogonal
	W_{Int}, interischiadic width between medial margins of ischia, minimum	Orthogonal
	D_{PrA}, preacetabular depth (of ala praeacetabularis), minimum	Orthogonal
	Δ_{TA}, transacetabular distance, minimum, between the iliopubic margin (concave) and the tip of antitrochanter	Defined point
	$Ø_{Ac}$, acetabular diameter, between the cranial wall and the caudal rim of the acetabulum§	Defined point
Femur (Fig. 1D)	L_T, total length, perpendicular to the straight between the most proximal points of the capitulum and trochanter	Orthogonal
	L_M, medial length, maximum between the caput and the most distal point of the medial condyle	Defined point
	L_L, lateral length between the trochanter and the lateral condyle, maximum	Defined point
	$Ø_H$, head diameter, craniocaudal, in a transverse plane of the bone	Orthogonal
	$Ø_C$, corpus least (minimum) diameter, in a transverse plane of the bone	Orthogonal
	W_D, distal width, maximum, between the medial condyle and fibular semicondyle	Defined point
	W_P, proximal width, maximum, between the head and the outermost margin of the trochanter	Defined point
	$Ø_{CM}$, medial condyle diameter (oblique to the long axis of the femur)	Orthogonal
Tibiotarsus (Fig. 1E)	L_{IA}, interarticular length	Orthogonal

Table 1. Continued

Bone	Abbreviation and definition	Type
	W_C, corpus minimum width (distally)	Orthogonal
	D_C, corpus depth, minimum (immediately above the impressio ligamenti collateralis medialis longi), perpendicular to the flat cranial surface	Orthogonal
	W_P, proximal width, perpendicular to the long axis of the bone	Orthogonal
	D_P, proximal depth (including cranial cnemial crest) perpendicular to the long axis of the bone	Orthogonal
	W_D, distal width as measured cranially, perpendicular to the plane of the margin of the lateral condyle	Orthogonal
	D_{MD}, medial distal depth, perpendicular to the long axis of the bone	Orthogonal
	D_{LD}, lateral distal depth, perpendicular to the long axis of the bone	Orthogonal
Fibula (Fig. 1F)	D_C, corpus depth, maximum, across the iliofibular tubercle, perpendicular to the distal tibial facet	Orthogonal
	D_H, head depth, maximum, perpendicular to the caudal margin of the head (oblique to the long axis of the bone) across the tibial tuberosity	Orthogonal
	W_C, corpus width, minimum, in the narrowest part between the head and distal tibial facet, perpendicular to the long axis of the bone	Orthogonal
Tarsometatarsus (Fig. 1G)	L_T, total length	Orthogonal
	W_C, corpus width, minimum as determined by at least three trials at different locations	Orthogonal
	D_C, corpus depth, minimum (distally)	Orthogonal
	W_P, proximal width	Orthogonal
	D_{MP}, medial proximal depth	Orthogonal
	D_{LP}, lateral proximal depth (includes the protuberances for the lateral collateral ligament and fibularis brevis muscle)	Orthogonal
	Δ_{IFA}, dorsal interforaminal distance, maximum between the outer margins of dorsal (proximal vascular) foramina	Defined point
	Δ_{IFP}, plantar interforaminal distance between the inner margins of plantar (proximal vascular) foramina, minimum	Defined point
	W_{TD}, trochlea III distal width, taken conformably (perpendicular to the parallel planes of both trochlear labra)	Orthogonal
	$Ø_{TL}$, trochlea III lateral labrum diameter	Orthogonal
Pedal digit III phalanx 1 (Fig. 1H)	L_T, total length perpendicular to and extending from the straight connecting the trochlear apices to the ventral basis (with flexor tubercles)	Orthogonal
	L_D, dorsal length between the apex of the dorsal cotylar labrum and the distal midpoint of the trochlea	Defined point
	L_M, medial length, between the medial margin of the cotyla and the apex of the medial trochlear labrum	Defined point
	L_L, lateral length, between the lateral margin of the cotyla (at the mid-depth) and the apex of the lateral trochlear labrum	Defined point
	W_C, corpus width, minimum	Orthogonal
	D_C, corpus depth, minimum, perpendicular to the ventral surface immediately distal to the ligament scars	Orthogonal
	W_P, proximal width (between the cotylar margins, exclusive of the lateral insertional protuberances)	Orthogonal
	D_P, proximal depth (including the dorsal and ventral insertional protuberances), perpendicular to the straight between the tips of flexor tubercles	Orthogonal
	W_T, trochlear width, ventrally	Orthogonal
	D_T, trochlear mid-depth (at the midline)	Orthogonal
	D_{MT}, medial trochlear depth, across the medial labrum	Orthogonal

Table 1. Continued

Bone	Abbreviation and definition	Type
Pedal digit III phalanx 2 (Fig. 1I)	L_T, total length, between (and perpendicular to) the straight connecting the trochlear apices and the ventral cotylar labrum	Orthogonal
	L_D, dorsal length between the apex of the dorsal cotylar labrum and the distal midpoint of the trochlea	Defined point
	L_M, medial length between medial margin of the cotyla and apex of medial trochlear labrum	Defined point
	L_L, lateral length, between lateral margin of the cotyla and apex of lateral trochlear labrum	Defined point
	W_C, corpus width, minimum	Orthogonal
	D_C, corpus depth, minimum	Orthogonal
	W_P, proximal width (between the cotylar margins, exclusive of the lateral insertional protuberances)	Orthogonal
	D_P, proximal depth perpendicular to the ventral labrum	Orthogonal
	W_A, apical width, between the trochlear apices (as seen in dorsal view)	Defined point
	W_F, foveal width, minimum between the inner margins of the foveae ligg. collaterales¶	Defined point
	W_T, trochlear width, ventral, perpendicular to the medial labrum	Orthogonal
	D_T, trochlear mid-depth, in the midline	Orthogonal
Pedal digit III phalanx 3 (as in Fig. 1I)	L_T, total length, between (and perpendicular to) the straight connecting the trochlear apices and the ventral cotylar labrum	Orthogonal
	L_D, dorsal length between the apex of the dorsal cotylar labrum and the midpoint of the trochlea	Defined point
	L_M, medial length between medial margin of the cotyla and apex of the medial trochlear labrum	Defined point
	L_L, lateral length between lateral margin of the cotyla and apex of the lateral trochlear labrum	Defined point
	W_P, proximal width (between the cotylar margins, exclusive of the lateral insertional protuberances)	Orthogonal
	D_P, proximal depth perpendicular to the ventral labrum	Orthogonal
	W_T, trochlear width, maximum, ventrally between the proximal ends of the trochlear labra	Defined point
	W_A, apical width between the trochlear apices (in dorsal view)	Defined point
	W_F, foveal width, minimum, between the inner margins of the foveae ligg. collaterales	Defined point
	D_T, trochlear mid-depth, in the midline	Orthogonal
Pedal digit IV phalanges 1–4	As for pedal digit III	–

*This measurement should be accompanied by the count of synsacral vertebrae, which is variable.
†These two measurements correspond approximately to pre- and postacetabular lengths, which were not measured because the acetabulum does not offer a precise and convenient measurement point.
‡Lowe's (1931) 'span from outer ridge of one-antitrochanter to the other'.
§Close to Lowe's (1931) 'diameter at right angles' to the 'antitrochanteric diameter', the latter being imprecise because of the irregularities of the antitrochanteric rim of the acetabulum.
¶This measurement value may vary between the mid-length and the distal end of the fovea.

tibiotarsus and tarsometatarsus by 10–15%. The differences in size of pedal phalanges are larger, in the range of 15–18%, meaning that *S. c. syriacus* had relatively shorter and otherwise smaller toes. The only length measurement that is even lower (by 22–27%) in *S. c. syriacus* is that of the postacetabular pelvis, probably owing to incomplete ossification of its caudal end (Supporting Information, Table S4). Additionally, numerous transverse measurements are lower by ≥ 20%, including those of the scapulocoracoid, sternum and humerus (Supporting Information, Table S2), two depth values for the tibiotarsus (Supporting Information, Table S6), fibula (Supporting Information, Table S7), the corpus width of the tarsometatarsus (Supporting Information, Table S8) and three depths and width values for

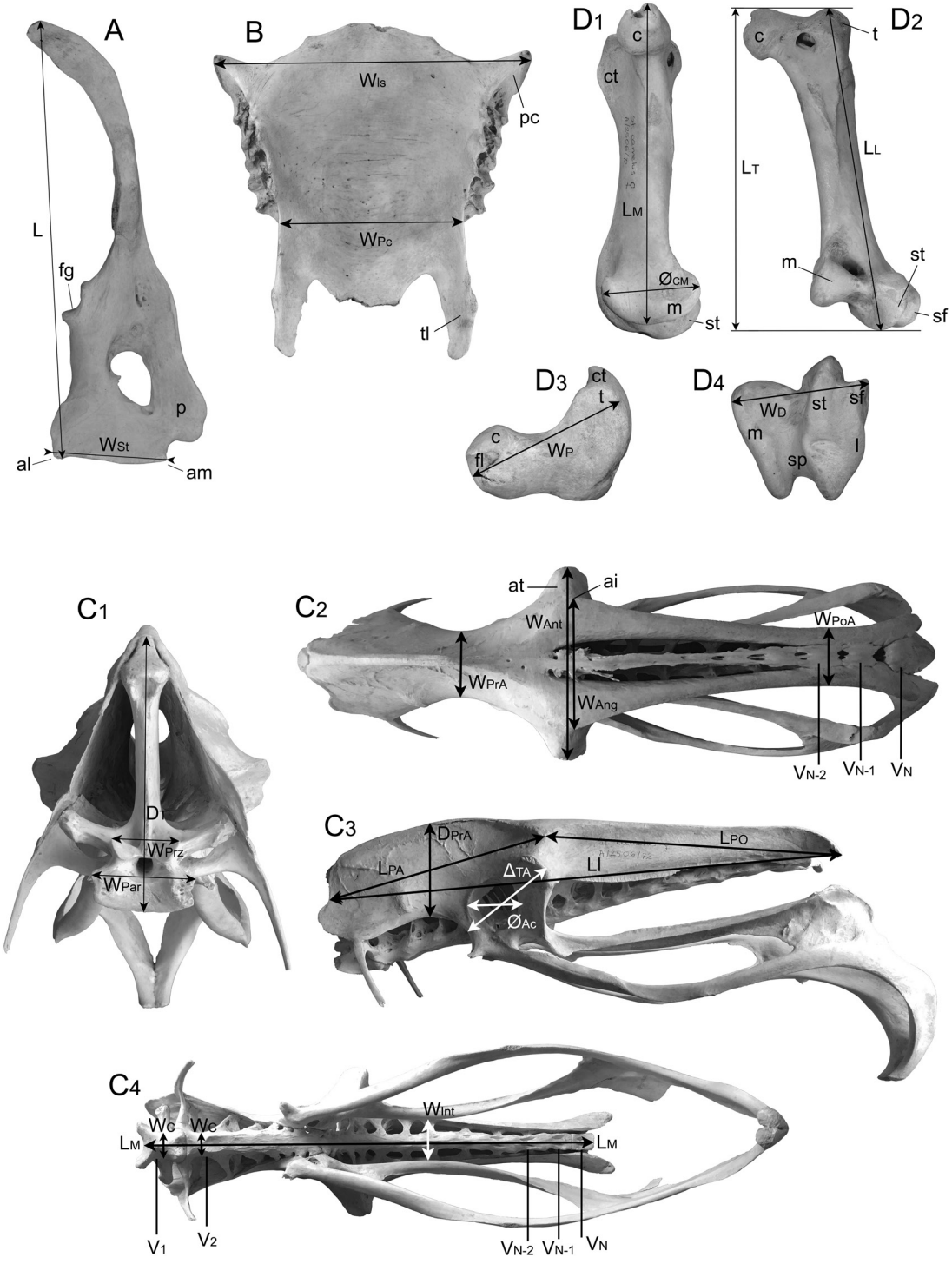

Figure 1. Graphical representations of measurements as defined in Table 1. A, scapulocoracoid in medial view. B, sternum in dorsal view. C, synsacrum and pelvis in cranial (C1), dorsal (C2), lateral (C3) and ventral (C4) view. D, femur in medial (D1), caudal (D2), proximal (D3 and distal (D4) view. E, tibiotarsus in cranial (E1) and medial (E2) view. F, fibula in cranial (F1), lateral (F2) and caudomedial (F3) view. G, tarsometatarsus in proximal (G1), dorsal (proximal end; G2), plantar (G3) and lateral (G4) view. H, phalanx 1 in dorsal (H1), ventral (H2), lateral (H3), medial (H4) and proximal (H5) view. I, pedal digit III phalanx 2 in dorsal (I1), ventral (I2) and medial (I3) view. Anatomical abbreviations: ai, angulus ilii; al, angulus lateralis; am, angulus medialis; at, antitrochanter; c, caput femoris; cc, crista cnemialis cranialis; cn, crista cnemialis lateralis; cp,

each phalanx 1 and 2 of pedal digit III (Supporting Information, Tables S9 and S10).

We also provide the first skeletal measurements for the hitherto questionable and largely dismissed taxon, *S. c. spatzi* (Supporting Information, Tables S2–S10). A single available specimen revealed a striking distinctness of its skeletal proportions. Most of its length dimensions place it between the living ostriches, beyond or at the minimum end of their ranges, and the much smaller Arabian ostriches. The wing bones of *S. c. spatzi* are consistently shorter (especially the carpometacarpus, less so phalanx 1 of the middle digit), but the distal width of the humerus is markedly greater than for the living ostriches. Most pelvic dimensions are below or barely approach the means for extant ostriches except for the greater (107–108%) width of the postacetabular pelvis, starting from the level of the acetabula. Most femoral dimensions are slightly below (91–97%) the means for the living ostriches except for the corpus diameter, which is distinctly smaller (86%, as in one specimen of *S. c. syriacus*), and the distal width, which is distinctly greater (109%) than in the living ostriches. The tibiotarsus is intermediate in length and in all other dimensions between *S. c. syriacus* and the living ostriches (Supporting Information, Table S6). In contrast, the tarsometatarsus is the same length as in *S. c. syriacus*, whereas its proximal and distal depths approach (96–99%) the means for the living ostriches (Supporting Information, Table S8). Pedal digit III phalanges approach or exceed the means for the living ostriches in length and, consistent with the tarsometatarsus, both proximal and distal depths (Supporting Information, Tables S9 and S10).

Struthio camelus spatzi was definitely smaller than any of the living ostriches. Stresemann (1927) referred to the three adult individuals (two males and one female) raised in Berlin Zoo as looking diminutive in comparison to a big male of *S. c. camelus*. In body mass, *S. c. spatzi* might have matched the Arabian ostrich, judging from the identical least diameter of the femoral corpus (Supporting Information, Table S5), or might have been larger, judging from the width and depth of the tarsometatarsal shaft, both of which are greater than in *S. c. syriacus* (Supporting Information, Table S8). Diameters of the femur and tarsometatarsus are considered to be equally reliable ($R^2 = 0.93$) for body mass estimates in birds (Field *et al.*, 2013), although the shape of the cross-section was shown to be less variable for the femoral compared with the tarsometatarsal corpus (Campbell & Marcus, 1992), which might lend more weight to the femoral corpus least diameter as an indicator of body mass in birds.

The unique proportions, especially the combination of short legs with big feet, differentiate *S. c. spatzi*, which is much more distinct from all other subspecies of *S. camelus* than the newly erected species, *S. molybdophanes*, which might possibly differ from *S. camelus* at the most by a longer scapulocoracoid (Fig. 2). We therefore confirm a separate taxonomic status of *S. c. spatzi*, at least as a subspecies, and propose the vernacular name 'highland ostrich'.

STRUTHIO CAMELUS SPATZI STRESEMANN, 1926, AMENDED

Struthio camelus spatzi Stresemann, 1926: 139.

Holotype: Egg, Museum für Naturkunde, Berlin, ZMB B.1180a (not examined).

Referred specimen: Adult male skeleton ZMB 36879 Stresemann, 1927: 135.

Remark: The skeleton ZMB 36879 comes from one of three birds, referred to by Stresemann (1927) as 'cotypes', kept at that time in Berlin Zoo.

Expanded diagnosis: Smaller than the living subspecies (with most dimensions 88–100%) except for the synsacrum (Supporting Information, Table S3), postacetabular pelvis (Supporting Information, Table S4), distal ends of the humerus (Supporting Information, Table S2), femur except for a smaller corpus diameter (Supporting Information, Table S5), and pedal phalanges III/1 and III/2 (Fig. 2; Supporting Information, Tables S9 and S10). Tarsometatarsus length < 440 mm (as in *S. c. syriacus*). The ratio of the length of tibiotarsus to tarsometatarsus is > 1.15, compared with 1.11–1.14 in extant ostriches. Phalanges III/1 and III/2 are as in extant ostriches, with the respective total lengths of ~90 mm (in the lower range of *S. c. camelus*) and 60 mm (as in *S. c. camelus*). The ratio of the length of tarsometatarsus to phalanx III/2 is 7.1, compared with 7.6–9.0 (8.0–9.0 for males) in extant ostriches. The pattern of egg pores of the

crista plantaris mediana; ct, crista trochanteris; dl, foramen dorsale laterale; dm, foramen dorsale mediale; em, epicondylus medialis; fd, facies tibialis distalis; ff, facies femoralis; fg, facies glenoidalis; fl, fovea ligmenti capitis; fm, foramen plantare mediale; fp, facies tibialis proximalis; fpl, foramen plantare laterale; il, impressio ligamenti collateralis medialis longi; l, condylus lateralis; ll, labrum laterale; lm, labrum mediale; m, condylus medialis; p, processus procoracoideus; pc, processus craniolateralis (sternocoracoideus); pm, foramen plantare mediale; sf, semicondylus fibularis; sp, sulcus patellaris; st, semicondylus tibiofibularis; t, trochanter; tf, tuberositas femoralis; ti, tuberculum m. iliofibularis; tIII, trochlea metatarsi III; tIV, trochlea metatarsi IV; tl, trabecula lateralis; tt, tuberositas tibialis. For explanation of measurement tags, see Table 1.

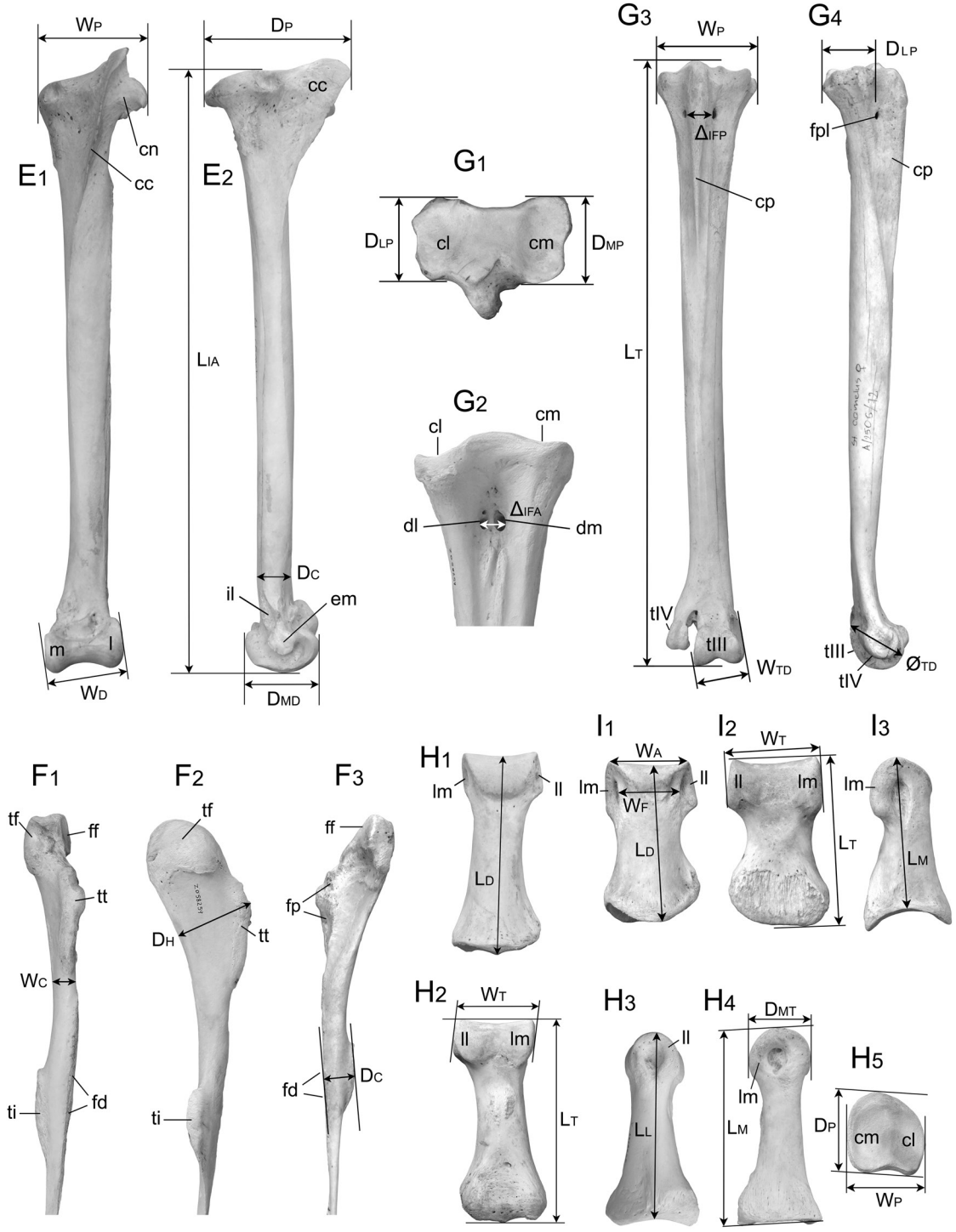

Figure 1. Continued.

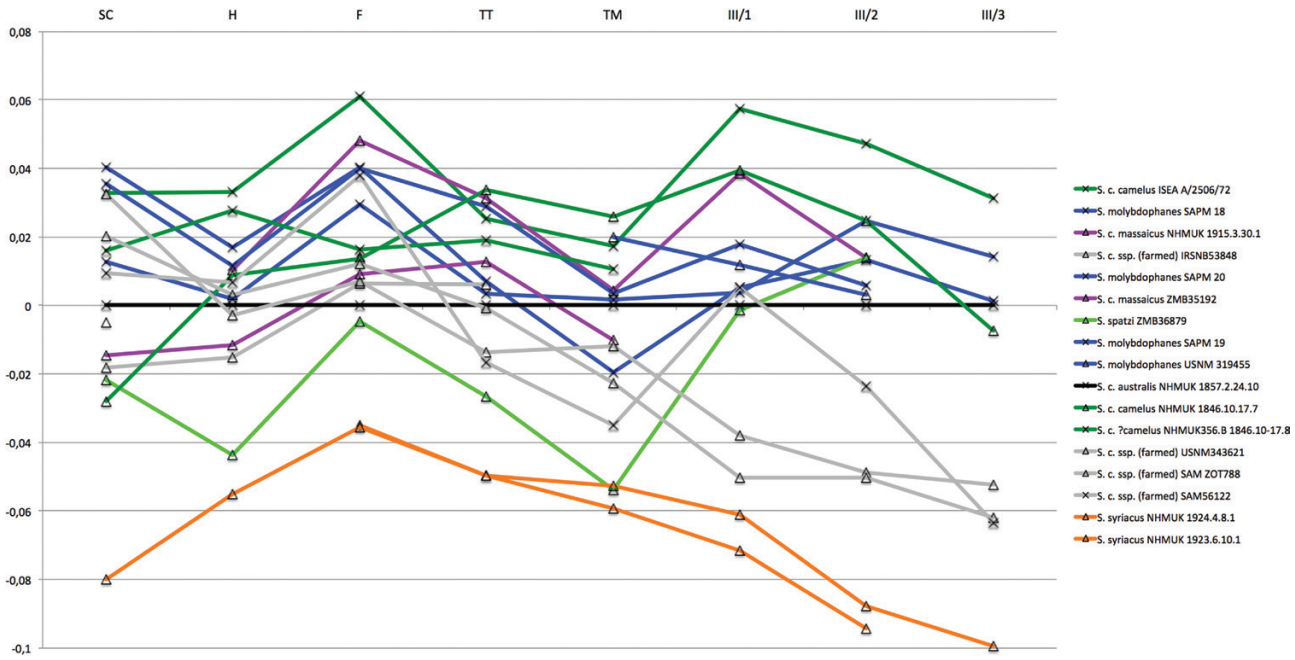

Figure 2. Simpson's ratio diagram comparing the lengths of scapulocoracoid (SC), humerus (H), femur (F), tibiotarsus (TT), tarsometatarsus (TM), and the first (III/1), second (III/2), and third (III/3) pedal digit III phalanges of living and extinct ostriches (Struthio), with *Struthio camelus australis* NHMUK 1857.2.24.10 as a reference (the black straight line at level 0). See the Supporting Information for the adopted lengths of limb segments (Table S17) and their LOG (decimal logarithmic) values (Table S18).

intermediate type is as described by Schönwetter (1927), Sauer (1968, 1972) and Mikhailov & Zelenkov (2020).

Skeletal variation and sexual dimorphism

Although the coefficients of variation of most measurements in the living ostriches do not exceed 6% (Supporting Information, Tables S2–S13), some of them are distinctly higher as a result of variable ossification (intrinsic variation) or, in addition, some indeterminacy owing to the absence of exact measurement points when taking minimum width or depth measurements across continuous surfaces. A high intrinsic variability affects single details, such as the sternal interspinal width (CV = 7.4), pelvic angular width (CV = 10.1), the cranial (CV = 8.5) and caudal (CV = 12.1) interforaminal distances of the tarsometatarsus and the proximal width between the cotylar margins of phalanx III/1 (CV = 7.1).

The indeterminacy and variability of measurement position might have contributed to the variation of the sternal postcostal width (CV = 9.6), pelvic postacetabular width (CV = 8.9), fibular corpus width (CV = 8.8), tarsometatarsal corpus depth (CV = 8.4) and many transverse measurements of phalanx III/2: corpus width (CV = 9.1), apical width (CV = 7.0), trochlear depth (CV = 7.1) and foveal width (CV = 7.1), with the foveal width also being highly variable in phalanx III/3 (CV = 9.5). The most variable and thus the least usable measurement turned out to be the interischiadic width (ischiadic span) of the pelvis (CV = 19.9), suggesting a strong intrinsic component of this variability in addition to the indeterminacy of the measurement point.

With a notable exception for the length of the tibiotarsus (Supporting Information, Table S6) and, especially, the tarsometatarsus (Supporting Information, Table S8), most measurement values (71 of 95 medians), including the transverse measurements of the tibiotarsus and tarsometatarsus, tend to be higher in females. However, the differences proved to be statistically significant or near-significant in only 14 measurements (Table 2). In ten of them, the ostrich females have consistently wider and/or deeper ends of limb bones, which suggests that the female skeleton (at least the appendicular skeleton) is more robust even if the males are taller owing to longer tarsometatarsi and tibiotarsi. Only three bones, namely the scapulocoracoid, humerus and pedal phalanx III/3, are significantly longer compared with males.

Table 2. Evidence of sexual dimorphism in the ostrich (*Struthio*) limb skeleton, including significant (*) and near-significant differences, as calculated from data in the Supporting Information (Tables S2–S13)

Measurement	Mann–Whitney *U*/*P*-value	Storer's index, median-based	Storer's index	Difference between medians[†] (%)
Scapulocoracoid total length	8/0.073	5.97	5.27	5.8
Humerus ventral length	8/0.073	2.61	3.52	2.6
Humerus distal width	5/0.019*	3.67	5.17	3.6
Femur proximal width	6/0.017*	9.15	8.0	8.75
Femur distal width	7.5/0.028*	8.59	6.93	8.2
Tibiotarsus medial distal depth	4/0.014*	10.03	6.53	9.55
Tarsometatarsus corpus depth	4/0.006*	14.36	10.33	13.4
Tarsometatarsus plantar interforaminal distance	7/0.026*	18.09	16.07	16.6
Tarsometatarsus trochlea III lateral labrum diameter	6.5/0.082	4.24	6.08	4.1
Pedal digit III phalanx 1 trochlear mid-depth	8/0.068	6.58	5.45	5.6
Pedal digit III phalanx 2 proximal depth	4.5/0.065	7.17	4.71	4.7
Pedal digit III phalanx 3 lateral length	0/0.057	13.78	12.91	12.9
Pedal digit IV phalanx 1 lateral trochlear depth	1/0.071	8.3	6.94	8.0
Pedal digit IV phalanx 1 trochlear mid-depth	0.071/0.036*	14.19	12.87	13.25

For the definitions of measurements, see Table 1 and Figure 1.
[†]As a percentage of the female median.

DISCUSSION

EXTINCT OSTRICHES

The Arabian ostrich, *S. c. syriacus*, has long been known as the smallest subspecies with the tarsometatarsus (measured as the tarsus) being 390–465 mm (average 420 mm) long compared with 450–530 mm (average 490 mm) reported for *S. c. camelus* (Vaurie, 1965). Our measurements of the tarsometatarsus (Supporting Information, Table S8), 426 mm for the fully ossified male *S. c. syriacus* in comparison to the mean of 487.3 mm for the living subspecies (492.5 mm for males only), are in perfect agreement with these data. In skeletal proportions, *S. c. syriacus* does not seem to differ substantially from the larger subspecies (Figs 2, 3), except for the relative shortness of the postacetabular pelvis, at 73–78% of the median length for the living subspecies compared with 84–96% for other pelvic measurements (Supporting Information, Table S4), and the relatively small size of pedal digit III, especially its phalanx 1 (Fig. 2; Supporting Information, Table S9).

The subspecies *S. c. spatzi* was erected by Stresemann (1926) for small ostriches from the southern part of the Western Sahara (historically known as the Rio de Oro area, between 26°N and 21°20′S). The diagnosis was based initially on the size of eight eggs (from various clutches) and the shape of eggshell pores, as later described in more detail by Schönwetter (1927). Four young ostriches were brought from the same area and placed in the Berlin Zoo. Three of them (two males and female) grew up by June 1927, were in good health, and yet looked dainty compared with a male *S. c. camelus* from Senegal (Stresemann, 1927). Unfortunately, there is no record of their skeletal measurements, which Stresemann (1927) intended to take.

Sauer (1968) has shown that the eggs assigned to *S. c. spatzi* by Schönwetter (1927) vary in shape and size, but the eggshells differ from *S. c. camelus* in the pore pattern, which reminds of a small mountain population of *S. c. australis* in south-western Africa. Sauer (1972: 42–43) envisioned the eggshell pore pattern of *S. c. spatzi* as intermediate between two widespread patterns of ostrich eggs, and thought that it 'must have evolved in a group of isolated birds aside from the mainstream of ostrich evolution'. This notwithstanding, the distinctiveness of *S. c. spatzi* has come to be denied. According to Brown *et al.* (1982: 33), both *S. c. spatzi* and *S. c. syriacus* merged through hybridization with *S. c. camelus*, but this seems to be pure speculation without any supporting evidence. Bertram (1985) asserted that 'the so called dwarf ostrich *S. c. spatzi* from Mauretania was

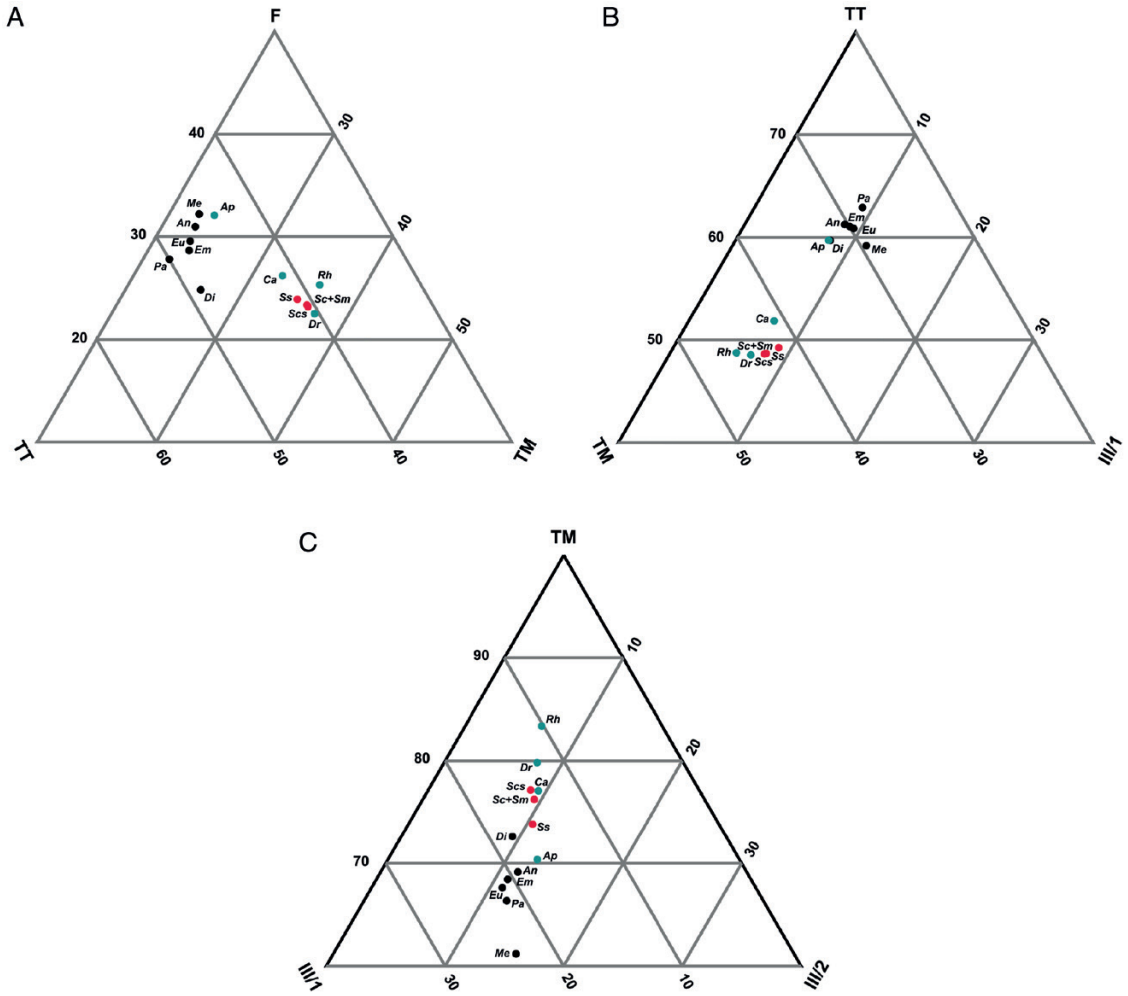

Figure 3. A, ternary diagrams comparing intramembral (length) proportions of femur (F) : tibiotarsus (TT) : tarsometatarsus (TM) in the extant ratites and moas. Data for *Struthio* are from the present work; for other ratites from Dickison (2007). See Supporting Information (Table S19) for the ternary ratios shown in the diagram. B, ternary diagrams comparing intramembral (length) proportions of tibiotarsus (TT) : tarsometatarsus (TM) : pedal digit III phalanx 1 (III/1) in the extant ratites and moas. Data for *Struthio* are from the present work; for other ratites from Dickison (2007) for the tibiotarsus and tarsometatarsus and from Farlow *et al.* (2013) for the phalanx. See Supporting Information (Table S20) for the ternary ratios shown in the diagrams. C, ternary diagrams comparing intramembral (length) proportions of tarsometatarsus (TM) : pedal digit III phalanx 1 (III/1) : pedal digit III phalanx 2 (III/2) in the extant ratites and moas. Data for *Struthio* are from the present work; for other ratites from Dickison (2007) for the tarsometatarsus and from Farlow *et al.* (2013) for the phalanges. See Supporting Information (Table S21) for the ternary ratios shown in the diagrams. Point labels: *An*, *Anomalopteryx didiformis*; *Ap*, *Apteryx* (the mean for *Apteryx australis*, *Apteryx mantelli* and *Apteryx oweni*); *Ca*, *Casuarius* (the mean for *Casuarius casuarius*, *Casuarius unappendiculatus* and *Casuarius bennetti*); *Di*, *Dinornis* (the mean for *Dinornis robustus* and *Dinornis novaezealandiae*); *Dr*, *Dromaius novaehollandiae*; *Em*, *Emeus crassus*; *Eu*, *Euryapteryx curtus* (the mean for *Euryapteryx curtus curtus* and *Euryapteryx curtus gravis*); *Me*, *Megalapteryx didinus*; *Pa*, *Pachyornis* (the mean for *Pachyornis australis*, *Pachyornis elephantopus* and *Pachyornis geranoides*; *Rh*, *Rhea* (the mean for *Rhea americana* and *Rhea pennata*); *Sc*, *Struthio camelus* (the mean for *Struthio camelus australis*, *Struthio camelus camelus* and *Struthio camelus massaicus*); *Sc+Sm*, the mean for *Struthio camelus* and *Struthio molybdophanes*; *Scs*, *Struthio camelus syriacus*; *Ss*, *Struthio camelus spatzi*.

mistakenly classified on inadequate information'. Folch (1992) referred to the subspecies *S. c. spatzi* as of 'doubtful validity', and recently, Folch *et al.* (2020) deemed differences in the eggshell to be attributable to individual variation. However, a recent detailed study by Mikhailov & Zelenkov (2020) confirmed the

distinctiveness and intermediate status of the eggshell pore pattern in *S. c. spatzi* between non-specialized and specialized struthioid types, essentially as put forward by Sauer (1972).

The referred skeleton ZMB36879 of *S. c. spatzi* differs from all other ostriches in having a short tarsometatarsus, of nearly identical length to otherwise smaller *S. c. syriacus* (Fig. 1; Supporting Information, Table S8), i.e. 86–88% of the mean of extant ostriches, and a big pedal digit III, as big or, it appears, slightly bigger than in the living ostriches, 93–105% of the means for the living ostriches (Fig. 1; Supporting Information, Tables S9 and S10). The large size of the third toe is correlated with the striking enlargement of the femur at the distal end (Supporting Information, Table S5), which provides the origins for the toe flexors (Gangl *et al.*, 2004; Smith *et al.*, 2006). Although some of their tendons attach in the popliteal fossa, which may or may not influence the femoral distal width, the thick tendon of origin of the powerful musculus flexor perforatus digiti III (which itself provides the place for the origin of m. flexor perforatus digiti IV) attaches to the lateral condyle of the femur and thus might influence its size.

In terms of the leg intramembral proportions femur : tibiotarsus : tarsometatarsus and tibiotarsus : tarsometatarsus : digit III phalanx 1, *S. c. spatzi* is separated from all other ostriches (including *S. c. syriacus*) by the same distance as from *Dromaius novaehollandiae* (Latham, 1790), and in terms of tarsometatarsus : digit III phalanx 1 : digit III phalanx 2 proportions, *S. c. spatzi* stands midway between the living flightless palaeognaths (including the ostriches) and the moas, being equidistant from *Dinornis* (Owen, 1843) and other ostriches (Fig. 3). These differences in skeletal proportions make the separate subspecies status of *S. c. spatzi* much better supported than the currently accepted species status of *S. molybdophanes*, which is not supported by the intramembral proportions in the leg. There is no slightest reason to believe that the recorded differences, such as the relatively short tarsometatarsus and long toes, represent an anomaly resulting from rearing conditions, inasmuch as leg deformities in farmed ostriches have been given special attention (Mushi *et al.*, 1999), and no such differences are known from numerous ostrich skeletons in museum collections, most of which come from captive birds.

The lengths of the shank and tarsus jointly determine the maximum stride length in birds (Alexander, 1977; Jones *et al.*, 2000). With the longest tibiotarsus and tarsometatarsus of all birds, the living ostriches are the fastest avian runners, having a stride length ≤ 5 m (Schaller *et al.*, 2011). However, in *S. c. spatzi* both the tibiotarsus and, especially, the tarsometatarsus are shorter by 8 and 12%, respectively, compared with the living ostriches (Supporting Information, Tables S6 and S8), whereas the bones supporting the trunk, including the scapulocoracoid, sternum and, especially, the pelvis, are much closer or, in the case of the synsacrum, match or exceed in size the living ostriches (Supporting Information, Tables S2–S4). This indicates that the highland ostriches must have been slower than the living ostriches, which might have contributed to their demise. In north-western Africa, the ostriches were 'hunted on horseback, having first been tracked until within sight and then chased until cornered' (Davies, 2002: 57).

Long legs or, more precisely, a greater 'hip height', impose less stability (Hildebrand, 1985; Zeffer *et al.*, 2003), which can be compensated by a larger foot span (Hildebrand, 1985). Recent studies confirm that the mechanics of running across rough terrain are similar in all terrestrial birds independent of size (Birn-Jeffrey *et al.*, 2014) and involve adjustments of limb angle (Daley & Biewener, 2006), thus conveying significance to differences in the length of toes. According to Stresemann's (1926, 1927) informers, *S. c. spatzi* inhabited a vast area that covered a part of the Atlas Mountains in Morocco and the hamadas or rocky deserts (regs), with a pronounced relief and steep escarpments (Fairbridge, 1968), as in a part of the Western Sahara today. These landscapes are different from those inhabited by most living ostriches and certainly impose special requirements for locomotion, especially regarding manoeuvrability and balance. We therefore propose that these ostriches were less cursorial and better adapted to rough terrain of rocky highlands, hence the proposed vernacular name, 'highland ostrich'. Consistent with this interpretation is the similarity of the eggshell pore patterns in *S. c. spatzi* to those of an isolated mountain population of *S. c. australis* (Sauer, 1968).

The unique foot proportions in *S. c. spatzi* must have had significant biomechanical consequences because they affect the action of the ankle (metatarsophalangeal) joint, which in ostriches, unlike other birds, is elevated above the ground. Pedal digit III supports the majority of the load (Schaller *et al.*, 2011), and its (plantar) flexion provides the main propulsive force (Hutchinson, 2004; Smith *et al.*, 2006). The metatarsophalangeal III/1 joint acts as a shock absorber and elastic energy store (Rubenson *et al.*, 2011; Schaller *et al.*, 2011), and its action differs between walking and running on a solid substrate (Zhang *et al.*, 2017), but not on sand (Zhang *et al.*, 2018), which supports our hypothesis that the unique foot proportions in *S. spatzi* evolved as an adaptation to the rugged landscapes of north-western Africa.

In the foot proportions, especially in the relative lengths of pedal digit III and the tarsometatarsus, *S. c. spatzi* (Fig. 2) seems to be paralleled among moas

by *Megalapteryx didinus* (Owen, 1883), a relatively small (~21 kg) species that inhabited 'high country' of the South Island of New Zealand (Worthy & Scofield, 2012) up to ≥ 1800 m a.s.l. (Atkinson & Greenwood, 1989) and seems to have had limited locomotory power compared with other moas (Kooyman, 1991). Thus, *S. c. spatzi* and *M. didinus* seem to provide another example of adaptive counterparts that evolved independently in similar, geographically separated habitats. All other moas have pedal digit III smaller than in *M. didinus*, whose foot also shows similarities to that of kiwis, *Apteryx* Shaw, 1813 (Farlow *et al.*, 2013). This raises a possibility that the enlargement of pedal digit III, especially its phalanx 2, and the relative shortening of the tarsometatarsus evolved in *S. c. spatzi* and *M. didinus* in response to the same demand of maintaining greater stability in the rugged habitat.

Skeletal variation and sexual dimorphism

Intraspecies metric variation in the skeleton of Neognathae is usually in the range of 2–6% (Schneider & Dunn, 1924; Larson, 1930; Engels, 1938; Simpson, 1946; Bährmann, 1970, 1974; Lidauer, 1982; Solti, 1996), with CVs higher for the transverse measurements of the ends and shafts compared with the lengths of bones (Goodge, 1951; Ericson, 1987). The recorded variation in two closely related species of living ostriches (Supporting Information, Tables S2–S13) is higher than intraspecific variation in the neognath species, as one could expect from the taxonomic diversification of the set including three subspecies of *S. camelus* and *S. molybdophanes*. However, it is unexpectedly lower than in two species of other living flightless palaeognaths, the emu *Dromaius novaehollandiae* (Long, 1965) and, except for the distal widths of the femur and tarsometatarsus, the kiwi, *Apteryx australis* Shaw, 1813 (Cracraft, 1976). It is also much lower than for the 'expanded species' of the moas as defined by (Cracraft, 1976). Aside from the problems of distinguishing species and sexing individuals of moas, now largely resolved through DNA analyses (Bunce *et al.*, 2003, 2009), the lower intraspecific variation recorded in our study might represent an artefact of using a set of better-defined measurements.

The scarcity of ostrich specimens with reliable subspecies identification (rather than farmed hybrids) does not permit a meaningful biometric comparison of the living species and subspecies. The subspecies of *S. camelus* and *S. molybdophanes* cluster together in the limb length and proportions except that all three *S. c. camelus* specimens have relatively the shortest scapulocoracoids, as does *S. c. syriacus* (Fig. 1), the closest relative of *S. c. camelus* (Miller *et al.*, 2011). However, the sample does provide reliable information on the range of variation among the living ostriches, which is essential for comparisons with fossils and the identification of numerous subfossil and archaeozoological finds. In addition, although the sample of sexed specimens is small, it contains specimens of heterogeneous origins, including wild, zoo and a few farmed specimens, which rules out any bias attributable to hunting, husbandry or farming practices. We therefore think that the use of non-parametric statistics warrants a meaningful test for differences between sexes.

The evidence of subtle sexual dimorphism we discovered in the ostrich skeleton is unexpected, because male ostriches are known to be slightly larger and heavier than females (e.g. Folch *et al.*, 2020) and yet the latter turn out to have most of their limb bones bulkier and a few of them slightly longer than in males. The dimorphism in ostrich skeletons turns out to be size independent and thus calls for a different explanation, which is likely to be found in the genetically determined covariance of morphological traits, known as morphological integration (Klingenberg, 2014). Eleven of 14 statistically significant (or nearly so) differences between sexes involve width and/or depth (Table 2), which makes our results consistent with the independence of longitudinal and transverse postcranial dimensions as established independently in the moas (Cracraft, 1976), anatids (Livezey & Humphrey, 1986), pigeons (Nemeschkal, 1999) and passerines (Power, 1971; Nemeschkal, 1999). The increased thickness of female limb bones might have evolved to enhance the storage of calcium in the skeleton for egg production or to compensate for the faster gains of body mass in female chicks (Mushi *et al.*, 1998). However, in the absence of comparable detailed osteological studies, it is unclear whether the same morphogenetic mechanism of global limb bone thickening is involved in sexual dimorphism in other birds.

The remaining three significant sexual differences are in the length of bones in two anatomically and thus morphogenetically widely isolated bones, the scapulocoracoid and humerus, and in pedal digit III phalanx 3 (Table 2). The covariation of the scapulocoracoid and humerus seems accountable in terms of the known proximodistal patterning of vertebrate limbs, including avian wings (Towers & Tickle, 2009), but other than that no published data on size-independent dimorphism of these bones are available.

Most of the pelvic limb bones do not show any distinct dimorphism in length, in agreement with Schaller *et al.* (2005), although the tarsometatarsus tends to be slightly longer in males (Supporting Information, Table S8). The dimorphic length of pedal digit III phalanx 3 might have gone unnoticed by Schaller *et al.* (2005)

because measurements of the entire digit III (i.e. of the assembled phalanges, including the variable ungual) necessarily lack the precision of measurements of single bones.

CONCLUSIONS

With all due caution commanded by a limited sample of selected skeletons, our analysis of a comprehensive set of 95 statistically usable measurements suggests subtle, size-independent sexual dimorphism in the skeleton of ostriches. Despite being smaller overall, females tend to have thicker limb bones (i.e. wider and/or deeper) than males. Such dimorphism is accountable in terms of the morphological integration (or covariance among characters) in the avian skeleton, where an independent regulation of the longitudinal and transverse dimensions of bones has been demonstrated. This subtle dimorphism might need to be taken into account when identifying numerous Neogene ostriches across Eurasia and Africa.

We validate the extinct subspecies *S. c. spatzi* from northwestern Africa, as distinguished by unique skeletal proportions, with relatively short wing bones, a broad pelvis, short tarsometatarsi and big feet, suggesting an adaptation for increased stability of locomotion in the rugged landscapes that are specific for this part of Africa. We also confirm the subspecies status of the Arabian ostrich, *S. c. syriacus*, which, in contrast to *S. c. spatzi*, is consistently smaller than the living ostriches by ~10–25% in all skeletal dimensions.

ACKNOWLEDGEMENTS

We are grateful to Z. Bocheński (Instytut Systematyki i Ewolucji Zwierząt, Kraków, Poland), J. Cooper and R. Prys-Jones [Natural History Museum (NHMUK), Tring, UK], D. Drinkrow, G. and M. Avery, D. Hamerton, T. Matthews, R. Smith, D. Stynder and K. van Willingh [Iziko South African Museum (SAM), Cape Town, South Africa], S. Frahnert [Museum für Naturkunde (ZMB), Berlin, Germany], H. Obermaier and B. Möllenkamp [Staatssammlung für Anthropologie und Paläoanatomie (SAPM), München, Germany] for facilitating access to their collections; Gilles Escarguel (LEHNA, France) for help with statistics; and A. Manegold (Staatliches Museum für Naturkunde, Karlsruhe, Germany) and F. Steinheimer (Martin-Luther-Universität Halle-Wittenberg, Halle (Saale), Germany) for their efforts to locate and access the specimens of *S. c. spatzi*.

A.E. was supported by Poland's Ministry of Science and Higher Education (grant number N303 549339). A.L. benefitted from a postdoctoral grant of the South African National Research Foundation/African Origins Platform/West Coast Fossil Park Initiative (Iziko South African Museum, Cape Town, South Africa), US National Science Foundation NSF grant 0321893 RHOI and Synthesys grant GBTAF-1341. We thank three anonymous reviewers and the Associate Editor for greatly improving our manuscript. The authors declare no conflicts of interest.

REFERENCES

Alexander RM. 1977. Terrestrial locomotion. In: Alexander RM, Goldspink G, eds. *Mechanics and energetics of animal locomotion*. London: Chapman and Hall, 168–203.

Atkinson IA, **Greenwood RM. 1989.** Relationships between moas and plants. *New Zealand Journal of Ecology* **12:** 67–96.

Bährmann U. 1970. Vergleichende osteologische Untersuchungen an *Sturnus vulgaris* L. und anderen Arten unter besonderer Berücksichtigung der Proportionierung der vorderen und hinteren Extremität. *Zoologische Abhandlungen Staatliches Museum für Tierkunde in Dresden* **31:** 12–38.

Bährmann U. 1974. Vergleichende osteometrische Untersuchungen an Rumpfskeletteilen und Extremitäten von einigen Tagraubvögeln aus den Familien Accipitridae, Pandionidae und Falconidae. *Zoologische Abhandlungen Staatliches Museum für Tierkunde in Dresden* **33:** 32–62.

Bertram BCR. 1985. Ostrich. In: Campbell B, Lack E, eds. *A dictionary of birds*. Arrington: Buteo Books, 416–417.

Birn-Jeffery AV, **Hubicki CM**, **Blum Y**, **Renjewski D**, **Hurst JW**, **Daley MA. 2014.** Don't break a leg: running birds from quail to ostrich prioritise leg safety and economy on uneven terrain. *The Journal of Experimental Biology* **217:** 3786–3796.

Brown LH, **Urban EK**, **Newman K. 1982.** *The birds of Africa*, **Vol. 2**. London: Academic Press.

Berns CM, **Adams DC. 2010.** Bill shape and sexual shape dimorphism between two species of temperate hummingbirds: black-chinned hummingbird (*Archilochus alexandri*) and ruby-throated hummingbird (*A. colubris*). *The Auk* **127:** 626–635.

Bunce M, **Worthy TH**, **Ford T**, **Hoppitt W**, **Willerslev E**, **Drummond A**, **Cooper A. 2003.** Extreme reversed sexual size dimorphism in the extinct New Zealand moa *Dinornis*. *Nature* **425:** 172–175.

Bunce M, **Worthy TH**, **Phillips MJ**, **Holdaway RN**, **Willerslev E**, **Haile J**, **Shapiro B**, **Scofield RP**, **Drummond A**, **Kamp PJ**, **Cooper A. 2009.** The evolutionary history of the extinct ratite moa and New Zealand Neogene paleogeography. *Proceedings of the National Academy of Sciences of the United States of America* **106:** 20646–20651.

Burchak-Abramovich NI. 1953. Iskopayemyye strausy Kavkaza i yuga Ukrainy [Fossil ostriches of Caucasus and southern Ukraine]. *Trudy Estestvenno-istoricheskogo Muzeya imeni G. Zardabi* **7:** 1–206.

Campbell KEJ, **Marcus L. 1992.** The relationship of hindlimb bone dimensions to body weight in birds. *Science Series, Natural History Museum of Los Angeles County* **36:** 395–412.

Cracraft J. 1976. Covariation patterns in the postcranial skeleton of moas (Aves, Dinornithidae): a factor analytic study. *Paleobiology* **2:** 166–173.

Cramp S, **Simmons KEL. 1977.** The birds of the Western Palearctic. Vol. 1. Ostrich to ducks. In: *Handbook of the birds of Europe, the Middle East and North Africa*. Oxford: Oxford University Press.

Daley MA, **Biewener AA. 2006.** Running over rough terrain reveals limb control for intrinsic stability. *Proceedings of the National Academy of Sciences of the United States of America* **103:** 15681–15686.

Davies SJJF. 2002. *Ratites and tinamous*. Oxford, New York: Oxford University Press.

Davison GWH. 1985. Avian spurs. *Journal of Zoology* **206:** 353–366.

Del Hoyo J, **Collar NJ. 2014.** *HBW and BirdLife International illustrated checklist of the birds of the world, Vol. 1: non-passerines*. Barcelona: Lynx Edicions.

Dickison MR. 2007. *The allometry of giant flightless birds*. Unpublished D. Phil. Thesis, Duke University.

Engels WL. 1938. Variation in bone length and limb proportions in the coot (*Fulica americana*). *Journal of Morphology* **62:** 599–607.

Ericson PG. 1987. Osteology of the eider *Somateria mollissima* (L.). A study of sexual, geographic and temporal morphometric variation in the eider skeleton. *The Museum of National Antiquities, Stockholm Studies* **5:** 1–142.

Fairbridge RW. 1968. Hamada, reg, serir, gibber, saï. In: *Geomorphology. Encyclopedia of earth science*. Berlin, Heidelberg: Springer.

Farlow JO, **Holtz TR**, **Worthy TH**, **Chapman RE. 2013.** Feet of the fierce (and not so fierce): pedal proportions in large theropods, other non-avian dinosaurs, and large ground birds. In: *Tyrannosaurid paleobiology*. Bloomington: Indiana University Press, 88–132.

Field DJ, **Lynner C**, **Brown C**, **Darroch SA. 2013.** Skeletal correlates for body mass estimation in modern and fossil flying birds. *PLoS One* **8:** e82000.

Folch A. 1992. Order Struthioniformes. In: Del Hoyo J, Elliott A, Sargatal J, eds. *Handbook of the birds of the world*, **Vol. 1**. Barcelona: Lynx Edicions, 76–110.

Folch A, **Christie DA**, **Jutglar F**, **Garcia EFJ. 2020.** Common ostrich (*Struthio camelus*), version 1.0. In: del Hoyo J, Elliott A, Sargatal J, Christie DA, de Juana E, eds. *Birds of the world*. Ithaca: Cornell Lab of Ornithology.

Frith CB. 1997. Huia (*Heteralocha acutirostris*: Callaeidae)-like sexual bill dimorphism in some birds of paradise (Paradisaeidae) and its significance. *Notornis* **44:** 177–184.

Gangl D, **Weissengruber GE**, **Egerbacher M**, **Forstenpointner G. 2004.** Anatomical description of the muscles of the pelvic limb in the ostrich (*Struthio camelus*). *Anatomia, Histologia, Embryologia* **33:** 100–114.

Goodge W. 1951. Variation in skeletal measurements of the common murre. *Condor* **53:** 99–100.

Handley WD, **Chinsamy A**, **Yates AM**, **Worthy TH. 2016.** Sexual dimorphism in the late Miocene mihirung *Dromornis stirtoni* (Aves: Dromornithidae) from the Alcoota Local Fauna of central Australia. *Journal of Vertebrate Paleontology* **36:** e1180298.

Hammer Ø, **Harper DAT**, **Ryan PD. 2001.** PAST: paleontological statistics software package for education and data analysis. *Palaeontologia Electronica* **4:** art. 4.

Hildebrand M. 1985. Walking and running. In: Hildebrand M, Bramble DM, Liem KF, Wake DB, eds. *Functional vertebrate morphology*. Cambridge, London: The Belknap Press of Harvard University Press.

Hutchinson JR. 2004. Biomechanical modeling and sensitivity analysis of bipedal running ability. I. Extant taxa. *Journal of Morphology* **262:** 421–440.

Jones TD, **Farlow JO**, **Ruben JA**, **Henderson DM**, **Hillenius WJ. 2000.** Cursoriality in bipedal archosaurs. *Nature* **406:** 716–718.

Klingenberg CP. 2014. Studying morphological integration and modularity at multiple levels: concepts and analysis. *Philosophical Transactions of the Royal Society B: Biological Sciences* **369:** 20130249.

Kooyman B. 1991. Implications of bone morphology for moa taxonomy and behavior. *Journal of Morphology* **209:** 53–81.

Lambert DM, **Shepherd LD**, **Huynen L**, **Beans-Picón G**, **Walter GH**, **Millar CD. 2009.** The molecular ecology of the extinct New Zealand Huia. *PLoS One* **4:** e8019.

Larson LM. 1930. Osteology of the California road-runner Recent and Pleistocene. *University of California Publications in Zoology* **32:** 409–428.

Leoni B, **Rubolini D**, **Romano M**, **di Giancamillo M**, **Saino N. 2008.** Avian hind-limb digit length ratios measured from radiographs are sexually dimorphic. *Journal of Anatomy* **213:** 425–430.

Lidauer RM. 1982. Die Variabilität von Längenmaßen und Gewicht an Skelettelementen der Singdrossel unter Berücksichtigung der Meßfehler. *Seevögel Zeitschrift des Vereins Jordsand zum Schutze der Seevögel* **1982:** 77–82.

Livezey BC, **Humphrey PS. 1986.** Flightlessness in steamer-ducks (Anatidae: Tachyeres): its morphological bases and probable evolution. *Evolution; international journal of organic evolution* **40:** 540–558.

Lowe PR. 1931. Struthious remains from northern China and Mongolia;with descriptions of *Struthio wimani*, *Struthio anderssoni*, and *Struthio mongolicus* spp. nov. *Palaeontologia Sinica* ser C **6**:1–47.

Mayr G. 2018. A survey of casques, frontal humps, and other extravagant bony cranial protuberances in birds. *Zoomorphology* **137:** 457–472.

McGillivray WB. 1985. Size, sexual size dimorphism, and their measurement in great horned owls in Alberta. *Canadian Journal of Zoology* **63:** 2364–2372.

Miller JM, **Hallager S**, **Monfort SL**, **Newby J**, **Bishop K**, **Tidmus SA**, **Black P**, **Houston B**, **Matthee CA**, **Fleischer RC. 2011.** Phylogeographic analysis of nuclear and mtDNA supports subspecies designations in the ostrich (*Struthio camelus*). *Conservation Genetics* **12:** 423–431.

Mikhailov KE, **Zelenkov N. 2020.** The late Cenozoic history of the ostriches (Aves: Struthionidae), as revealed by fossil eggshell and bone remains. *Earth Science Reviews* **208:** 103270.

Mushi EZ, **Binta MG**, **Chabo RG**, **Isa JFW**, **Phuti MS. 1999.** Limb deformities of farmed ostrich (Struthio camelus) chicks

in Botswana. *Tropical Animal Health and Production* **31:** 397–404.

Mushi EZ, **Isa JFW**, **Chabo RG**, **Segaise TT. 1998.** Growth rate of ostrich (*Struthio camelus*) chicks under intensive management in Botswana. *Tropical Animal Health and Production* **30:** 197–203.

Navarro C, **de Lope F**, **Møller AP. 2007.** Digit ratios (2D:4D), secondary sexual characters and cell-mediated immunity in house sparrows *Passer domesticus*. *Behavioral Ecology and Sociobiology* **61:** 1161–1168.

Nemeschkal HL. 1999. Morphometric correlation patterns of adult birds (Fringillidae: Passeriformes and Columbiformes) mirror the expression of developmental control genes. *Evolution; international journal of organic evolution* **53:** 899–918.

Olson VA, **Turvey ST. 2013.** The evolution of sexual dimorphism in New Zealand giant moa (*Dinornis*) and other ratites. *Proceedings of the Royal Society B: Biological Sciences* **280:** 20130401.

Petitte JN, **Davis G. 1999.** Breeding and genetics. In: Deeming DC, ed. *The ostrich: biology, production and health*. Wallingford: CAB International, 275–292.

Plumpton DL, **Lutz RS. 1994.** Sexual size dimorphism, mate choice, and productivity of burrowing owls. *The Auk* **111:** 724–727.

Power DM. 1971. Statistical analysis of character correlations in Brewer's blackbirds. *Systematic Zoology* **20:** 186–203.

Radford AN, **Du Plessis MA. 2004.** Extreme sexual dimorphism in green woodhoopoe (*Phoeniculus purpureus*) bill length: a case of sexual selection? *The Auk* **121:** 178–183.

Robinson TJ, **Matthee CA. 1999.** Molecular genetic relationships of the extinct ostrich, *Struthio camelus syriacus*: consequences for ostrich introductions into Saudi Arabia. *Animal Conservation* **2:** 165–171.

Rubenson J, **Lloyd DG**, **Heliams DB**, **Besier TF**, **Fournier PA. 2011.** Adaptations for economical bipedal running: the effect of limb structure on three-dimensional joint mechanics. *Journal of the Royal Society, Interface* **8:** 740–755.

Saino N, **Rubolini D**, **Romano M**, **Boncoraglio G. 2007.** Increased egg estradiol concentration feminizes digit ratios of male pheasants (*Phasianus colchicus*). *Die Naturwissenschaften* **94:** 207–212.

Sauer EGF. 1968. Calculations of struthious egg sizes from measurements of shell fragments and their correlation with phylogenetic aspects. *Cimbebasia A* **1:** 27–55.

Sauer EGF. 1972. Ratite eggshell and phylogenetic questions. *Bonner Zoologische Beiträge* **23:** 3–48.

Schaller NU, **D'Août K**, **Villa R**, **Herkner B**, **Aerts P. 2011.** Toe function and dynamic pressure distribution in ostrich locomotion. *The Journal of Experimental Biology* **214:** 1123–1130.

Schaller NU, **Herkner B**, **Prinzinger R. 2005.** Locomotor characteristics of the ostrich (*Struthio camelus*) I: morphometric and morphological analyses. In: *Proceedings of the 3rd International Ratite Science Symposium of the World's Poultry Science Association (WPSA) and 12th World Ostrich Congress, Madrid, Spain, 14–16 October 2005*. Beekbergen, The Netherlands: World Poultry Science Association (WPSA), 83–90.

Schneider M, **Dunn LC. 1924.** On the length and variability of the bones of the white leghorn fowl. *The Anatomical Record* **27:** 229–239.

Schönwetter M. 1927. Die Eier von *Struthio camelus spatzi* Stresemann. *Ornithologische Monatsberichte* **35:** 13–17.

Simpson GG. 1946. Fossil penguins. *Bulletin of the American Museum of Natural History* **87:** 1–99.

Smith NC, **Wilson AM**, **Jespers KJ**, **Payne RC. 2006.** Muscle architecture and functional anatomy of the pelvic limb of the ostrich (*Struthio camelus*). *Journal of Anatomy* **209:** 765–779.

Solti B. 1996. The comparative osteomorphological study of the European small-statured falcons (Aves: Falconidae). *Folia Historico Naturalia Musei Matraensis* **21:** 5–282.

Stewart JR. 2007. An evolutionary study of some archaeologically significant avian taxa in the Quaternary of the western Palaearctic. *British Archaeological Reports International Series* **1653:** 1–272.

Storer RW. 1966. Sexual dimorphism and food habits in tree North American accipiters. *Auk* **83:** 423–436.

Stresemann E. 1926. Die Vogelausbeute des Herrn Paul Spatz in Rio de Oro. *Ornithologische Monatsberichte* **34:** 137–139.

Stresemann E. 1927. Ueber die einstige Verbreitung von *Struthio camelus* in Algerien. *Ornithologische Monatsberichte* **35:** 135–136.

Sullivan MS, **Hillgarth N. 1993.** Mating system correlates of tarsal spurs in the Phasianidae. *Journal of Zoology* **231:** 203–214.

Temeles EJ, **Miller JS**, **Rifkin JL. 2010.** Evolution of sexual dimorphism in bill size and shape of hermit hummingbirds (Phaethornithinae): a role for ecological causation. *Philosophical Transactions of the Royal Society B: Biological Sciences* **365:** 1053–1063.

Towers M, **Tickle C. 2009.** Growing models of vertebrate limb development. *Development* **136:** 179–190.

Trombone T. 2013. *AMNH bird collection*. New York: American Museum of Natural History. Occurrence dataset doi:10.15468/xvzdcm accessed via GBIF.org on 5 March 2021.

Vaurie C. 1965. *The birds of the Palearctic Fauna / a systematic reference non-Passeriformes*. London: H.F. & G. Witherby.

Winde H. 1977. Vergleichende Untersuchungen über Proportionalität und Sexualdimorphismus im Skelett von *Asio otus otus* (L.) (Aves, Strigidae). *Zoologische Abhandlungen Staatliches Museum für Tierkunde in Dresden* **34:** 143–146.

Worthy TH, **Scofield RP. 2012.** Twenty-first century advances in knowledge of the biology of moa (Aves: Dinornithiformes): a new morphological analysis and moa diagnoses revised. *New Zealand Journal of Zoology* **39:** 87–153.

Zeffer A, **Johansson LC**, **Marmebro Å. 2003.** Functional correlation between habitat use and leg morphology in birds (Aves). *Biological Journal of the Linnean Society* **79:** 461–484.

Zhang R, **Ji Q**, **Han D**, **Wan H**, **Li X**, **Luo G**, **Xue S**, **Ma S**, **Yang M**, **Li J. 2018.** Phalangeal joints kinematics in ostrich (*Struthio camelus*) locomotion on sand. *PLoS One* **13:** e0191986.

Zhang R, **Ji Q**, **Luo G**, **Xue S**, **Ma S**, **Li J**, **Ren L. 2017.** Phalangeal joints kinematics during ostrich (*Struthio camelus*) locomotion. *PeerJ* **5:** e2857.

SUPPORTING INFORMATION

Additional Supporting Information may be found in the online version of this article at the publisher's web-site:

Table S1. Skeletal specimens of ostriches.
Table S2. Shoulder girdle and wing skeleton measurements (in millimetres) with statistics.
Table S3. Synsacrum measurements (in millimetres) with statistics.
Table S4. Pelvis measurements (in millimetres) with statistics.
Table S5. Femur measurements (in millimetres) with statistics.
Table S6. Tibiotarsus measurements (in millimetres) with statistics.
Table S7. Fibula measurements (in millimetres) with statistics.
Table S8. Tarsometatarsus measurements (in millimetres) with statistics.
Table S9. Pedal digit III phalanx 1 measurements (in millimetres) with statistics.
Table S10. Pedal digit III phalanx 2 measurements (in millimetres) with statistics.
Table S11. Pedal digit III phalanx 3 measurements (in millimetres) with statistics.
Table S12. Pedal digit IV phalanx 1 measurements (in millimetres) with statistics.
Table S13. Pedal digit IV phalanx 2 measurements (in millimetres) with statistics.
Table S14. Pedal digit IV phalanx 3 measurements (in millimetres) with statistics.
Table S15. Pedal digit IV phalanx 4 measurements (in millimetres).
Table S16. Digit III phalanx 4 (ungual) measurements (in millimetres).
Table S17. Lengths of segments used for the Simpson's diagram in Figure 2.
Table S18. LOG (decimal logarithmic) values of segment lengths in all taxa minus the respective logarithmic value for the living *Struthio camelus* subspecies, as used for Figure 2.
Table S19. Ternary ratios (as percentages) of femur (F) : tibiotarsus (TT) : tarsometatarsus (TM) in the living flightless palaeognaths and moas, as used for the ternary diagram in Figure 3A.
Table S20. Ternary ratios (as percentages) of tibiotarsus (TT) : tarsometatarsus (TM) : pedal phalanx III/1 in the living flightless palaeognaths and moas, as used for the ternary diagram in Figure 3B.
Table S21. Ternary ratios (as percentages) of tarsometatarsus (TM) : pedal phalanx III/1 : pedal phalanx III/2 in the living flightless palaeognaths and moas, as used for the ternary diagram in Figure 3C.